JOC The Journal of Organic Chemistry

ARTICLE

pubs.acs.org/joc

Stereolability of Dihydroartemisinin, an Antimalarial Drug: A Comprehensive Kinetic Investigation. Part 2

Walter Cabri,[†] Ilaria D'Acquarica,[‡] Patrizia Simone,[‡] Marta Di Iorio,[‡] Michela Di Mattia,[†] Francesco Gasparrini,[*,‡] Fabrizio Giorgi,[†] Andrea Mazzanti,[§] Marco Pierini,[*,‡] Marco Quaglia,[†] and Claudio Villani[‡]

[†]Analytical Development, R&D Department, Sigma-Tau S.p.A., Via Pontina km 30.400, 00040 Pomezia, Italy

[‡]Dipartimento di Chimica e Tecnologie del Farmaco, Sapienza Università di Roma, P. le Aldo Moro 5, 00185 Roma, Italy

[§]Dipartimento di Chimica Organica "A. Mangini", Università di Bologna, Viale Risorgimento 4, 40136 Bologna, Italy

Supporting Information

ABSTRACT: Artemisinin or *qinghaosu* has now largely given way to the more potent dihydroartemisinin (DHA, **1**) and its derivatives in the treatment of drug-resistant malaria, in combination with other classical antimalarial drugs. DHA is obtained by $NaBH_4$ reduction of artemisinin and contains a stereochemically labile center at C-10, which provided two lactol hemiacetal interconverting epimers, namely **1α** and **1*β***. In the solid state, the drug consists exclusively of the β-epimer; however, upon dissolution, the two epimers equilibrate, reaching different solvent-dependent ratios with different rates. Such equilibration also occurs in vivo, irrespective of the isomeric purity at which the drug would have been administered. The aim of this study was then to achieve an in-depth understanding of the kinetic features of the α/β equilibration. To this purpose, free energy activation barriers ($\Delta G^{\ddagger}$) of the interconversion were determined as a function of both general and specific acid and base catalysts, ionic strength, and temperature in different solvents by dynamic HPLC (DHPLC). In hydro-organic media, the dependence of $\Delta G^{\ddagger}$ on temperature led to the evaluation of the related enthalpic and entropic contributions. Theoretical calculations suggested that the rate-determining step of the interconversion is not the ring-opening of the cyclic hemiacetal but the previous reversible deprotonation of the individual epimers (base-catalyzed mechanism). The whole findings may contribute to shed some light on the mechanism of action and/or bioavailability of the drug at the molecular level.

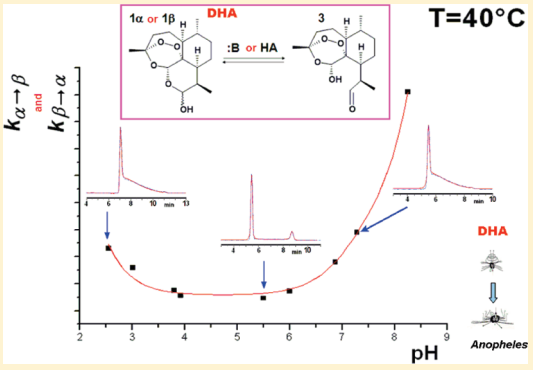

INTRODUCTION

Malaria is a mosquito-borne infectious disease caused by a eukaryotic protist of the genus *Plasmodium*. It is widespread in tropical and subtropical regions; each year, there are approximately 350−500 million cases of malaria, killing between one and three million people, the majority of whom are young children in sub-Saharan Africa.[1] In the past years, the combination of artemisinin derivatives with other antimalarial drugs (artemisinin-based combination therapies or ACTs) were developed and are now the treatment of choice for the most lethal forms of malaria.[2,3] Among such artemisinin derivatives, dihydroartemisinin (DHA, **1**), which is also its main metabolite, provides improved antimalarial potency.[3−5] DHA contains a stereochemically labile center at C-10, which provided two lactol hemiacetal interconverting epimers, namely **1α** and **1*β*** (Chart 1). The α-epimer bears the hydroxyl group in the equatorial position (absolute stereochemistry at C-10: *R*), and the β-epimer possesses an axial hydroxyl group.[6a] In the solid state, DHA consists exclusively of the β-epimer; however, upon dissolution, the two epimers equilibrate, reaching different solvent-dependent ratios with different rates. Such equilibration also occurs in vivo, irrespective of the isomeric purity at which the drug would have been administered. The intrinsic chemical instability of DHA was subject of investigation by several groups[6b−e] because it could prevent fulfillment of the internationally accepted stability requirements. Detailed studies on the chemical and stereochemical behavior of DHA should therefore have immediate relevance, inter alia, on all aspects related to drug formulation and bioequivalence analysis.

In the past, numerous HPLC methods[7−16] have been developed for the analysis and plasma level monitoring of **1**, but none of them considers the effects of epimer equilibration on the analytical response. Moreover, after a first study showing that interconversion of the two epimers occurred in a chromatographic time scale,[17] no other related papers appeared in the literature afterward. Only recently[18] was this issue considered to provide improved and reliable HPLC procedures suited for both separation and quantification of the **1α** and **1*β*** epimers in solution and in complex mixtures, under conditions of suppressed interconversion. In such a study, we

Received: December 2, 2010
Published: May 04, 2011

Chart 1. Chemical Structures of Dihydroartemisinin (DHA, 1) Epimers

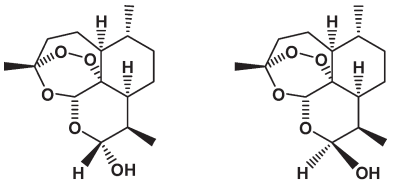

identified some optimal conditions (such as stationary phase and column temperature) able to minimize on-column epimerization while achieving the best selectivity and efficiency of separation. This paper, which is the second part of another focused on thermodynamic considerations,[19] deals with the kinetics of the **1β⇄1α** interconversion, with the aim of shedding light on the molecular factors involved into the mechanism of action and/or toxicity of the drug at molecular level.

RESULTS AND DISCUSSION

The very first study[17] showing that interconversion of the two DHA epimers occurred on a chromatographic time scale (i.e., on-column epimerization could be detected) was performed in 1986, but since then, no other related papers have appeared in the literature. In that study, the existence of the **1β⇄1α** epimerization was investigated at variable temperatures in aqueous−organic media (water−ethanol 55:45) by dynamic HPLC (DHPLC).[20] However, the author reported a largely overestimated activation energy barrier of 67.0 kcal mol^{-1} for the interconversion of the two DHA epimers, which cannot be related to dynamic events occurring on the chromatographic time scale at room temperature. We therefore recalculated by computer simulation[21] the rate constants from the published dynamic chromatograms[17] and found much lower energy barriers, actually consistent with those we recently reported within the same temperature range[18a] (see Figure 1S of the Supporting Information for a collection of the relevant superimposed experimental and simulated chromatograms). Nevertheless, such kinetic information did not provide a satisfactory picture of the process. In particular, the effects that a change of solvent, pH, ionic strength, and temperature may generate on the rate of the event were not investigated, and no information about the mechanism could be obtained. Such a scenario prompted a thorough kinetic investigation of the phenomena, with the aim of shedding some light on the mechanism of action and/or bioavailability of the drug at the molecular level.

Effect of pH, Ionic Strength, and Temperature on the Rate Constants. Owing to the biological activity of **1**, it is particularly significant to investigate the kinetic features of the **1β⇄1α** interconversion in aqueous media, which can be assimilated to biological fluids. Thus, we studied the epimerization in aqueous−organic mixtures as a function of both apparent pH and temperature and measured the relevant forward and backward rate constants by DHPLC (for details, see the Experimental Section). Chromatographic conditions were selected in order to achieve the best simulation of the relevant dynamic chromatograms with the lowest associated error.[18] All of the DHPLC experiments (examples of the obtained chromatograms are shown in Figure 1, superimposed with the relevant simulated traces) were carried out with a ternary mobile phase consisting of water−acetonitrile−methanol 55:35:10 (v/v/v) (hereafter denoted as WAM-solution) at controlled temperatures in the range of 10−70 °C.

Solutions of **1** in the mobile phase were buffered or not as needed to the apparent pH values (pH was measured in the ternary hydro-organic mixtures, while the electrode system was calibrated with aqueous standard buffers) ranging from 2.6 to 8.3 using 10 mM sodium phosphate. The measured first-order rate constants for the forward ($k_{\beta\rightarrow\alpha}$) and backward ($k_{\alpha\rightarrow\beta}$) interconversions (for details, see the Experimental Section) are reported in Table 1, whereas the corresponding free energy activation barriers have been calculated by the Eyring equation and are summarized in Tables 1Sa,b of the Supporting Information.

In principle, such rate constants may be expressed by the following general rate law, typical of hemiacetal breakdown[22]

$$k_{obs} = k_0 + k_H[H^+] + k_{OH}[OH^-] + \sum k_{HAi}[HA_i] + \sum k_{Ai}[A_i^-] \quad (1)$$

where k_{obs} generically represents the observed forward $k_{\beta\rightarrow\alpha}$ or backward $k_{\alpha\rightarrow\beta}$ first-order epimerization rate constants, k_H, k_{OH}, k_{HAi}, and k_{Ai} are the second-order rate constants for the process catalyzed by protons, hydroxide ions, general acids HA_i, and general bases A_i^-, whereas k_0 expresses the possible first-order rate constant for the spontaneous epimerization in the given medium. Because in the present case all the kinetic determinations were performed by DHPLC, the k_0 term will also include the catalytic contribution coming from the stationary phase (SPC) of the column here employed as the chromatographic separating tool. Such a value for the same commercial column (C_{18} symmetry, 3.5 μm; 75 × 4.6 mm i.d.) was already assessed in a previous study[18a] for both the forward β→α and backward α→β epimerizations of DHA (SPC = 1.10 × 10^{-3} and 4.68 × 10^{-4} s^{-1}, respectively). To get preliminary information on the potential contributions of ionic strength to k_{obs} we also carried out further DHPLC determinations of the $k_{\beta\rightarrow\alpha}$ and $k_{\alpha\rightarrow\beta}$ rate constants in the same mobile phase but containing, in place of phosphate, a catalytically inert salt (namely sodium chloride 1, 10, and 100 mM). The kinetic data obtained are collected in Table 1. Comparison of the rate constants obtained with or without phosphate buffer and salts (see Table 1) showed that ionic strength has negligible effects on the reaction rate, within the experimental error. This important result enabled us to directly use the measured first-order $k_{\beta\rightarrow\alpha}$ and $k_{\beta\rightarrow\alpha}$ rate constants (i.e., k_{obs} in eq 1) to analyze the role of protons and hydroxide ions, as well as that of H_3PO_4, $H_2PO_4^-$, and HPO_4^{2-} species as promoters of the epimerization. As an example, rate−pH profiles of the β→α epimerizations (i.e., the first-order rate constants values plotted as a function of pH) at four temperatures are reported in Figure 2. Inspection of the plots clearly indicates that the process is effectively catalyzed by both acid and basic species, reaching the minimum rate in the restricted pH range from 4.0 to 5.5. According to the general case expressed by eq 1, a more detailed form of dependence for k_{obs}, relative to the composition of the media employed as reacting solvent in the explored pH range, may be conveniently expressed by the following equation:

$$k_{obs} = k_0 + k_H[H^+] + k_{OH}[OH^-] + k_{H_3PO_4}[H_3PO_4] + k_{H_2PO_4^-}[H_2PO_4^-] + k_{HPO_4^{2-}}[HPO_4^{2-}] \quad (2)$$

Thus, in order to split out the contributions of each catalytic species from the k_{obs} data we performed new dedicated DHPLC

dx.doi.org/10.1021/jo102392p |J. Org. Chem. 2011, 76, 4831–4840

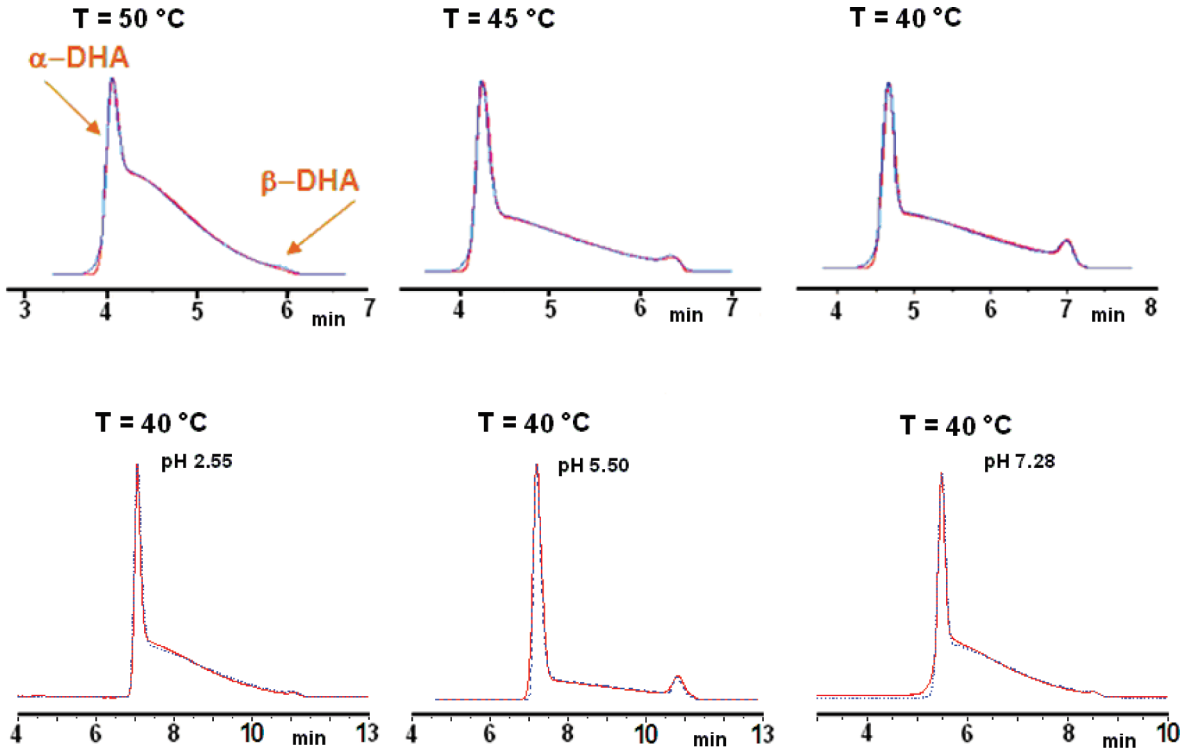

Figure 1. Superimposed experimental (red line) and simulated (blue line) dynamic chromatograms of **1** dissolved in mobile phase. Column: C_{18} symmetry, 3.5 μm (75 × 4.6 mm i.d.). Eluent: water−acetonitrile−methanol 55:35:10 (v/v/v). Flow rate: 1.0 mL min^{-1}. Detection: UV at 214 nm. The mobile phase was not buffered (top chromatograms) or buffered by 10 mM sodium phosphate to pH 2.55, 5.50, and 7.28 (bottom chromatograms).

determinations specifically created to quantify the input due to the buffer's components H_3PO_4, $H_2PO_4^-$, and HPO_4^{2-}. For this purpose, rate constant measurements at the selected temperature of 40 °C were repeated at seven established pHs (and then at seven different ratios $[A_i^-]/[HA_i]$) by progressively increasing the buffer concentration inside the range 10−200 mM (see Table 2S of the Supporting Information). The obtained dynamic chromatograms, reported in Figure 2S of the Supporting Information, clearly evidence the existence of active general catalysis by the buffer, which significantly increases on reduction of pH. According to the mathematical methods extensively described within the Supporting Information, it was possible to evaluate the second-order rate constants $k_{H_3PO_4}$, $k_{H_2PO_4^-}$, and $k_{HPO_4^{2-}}$ for the forward and backward epimerization of **1**. It is known that addition of organic modifiers to water solutions leads to an increase of both pH of the media and ionization constants (pK_a) of neutral and anionic acid species, as well as also of the solvent autoprotolysis constant value (pK_w) related to the employed water−organic mixture.[22] While effects produced by addition of methanol or acetonitrile to water solutions have been extensively investigated,[22a,b] no equivalent data are available for ternary mixtures in the literature. In addition, whereas changes of ionization constant for the dihydrogen phosphate anion (i.e., pK_{a2}) can be estimated according to detailed procedures reported for the limited case of binary mixtures involving either methanol[22c] or acetonitrile[22d,e] as the cosolvent, no equivalent information may be found about the first stage of ionization of the orthophosphoric acid (i.e., pK_{a1}). Thus, to perform evaluations of the above-cited second-order rate constants in WAM-solution, we resorted to the following approximations: (1) all changes of the involved solute ionization and solvent autoprotolysis constants (i.e., changes of the constants pK_{a1}, pK_{a2}, and pK_w) were calculated according to the procedure described[22d] for the transition from water to the binary aqueous−organic solution water−acetonitrile 65:35 (v/v), hereafter denoted as WA solution (that is to say, a mixture composition quite similar to that of the used ternary WAM-solution); (2) the increment suffered by the pK_{a1} constant in pure acetonitrile was roughly estimated by considering the typical changes reported for the first stage of ionization of other polyprotic acids, (i.e., tartaric and citric acid).[22d] From this, the relevant value in WA solution was also estimated (a detailed description of the whole procedure is reported in the Supporting Information). As a reference, the same rate constants were also evaluated by resorting to pK_{a1}, pK_{a2}, and pK_w in pure water. All of the relevant values were collected in Table 3S of the Supporting Information. Information on these data allowed us to correct the experimental k_{obs} constants by subtracting from their values the calculable buffer contributions at each relevant pH (i.e., the amounts $k_{H_3PO_4[H3PO4]}$, $k_{H_2PO_4^-}[H_2PO_4^-]$, and $k_{HPO_4^{2-}}[HPO_4^{2-}]$). The so elaborated new rate constants, k'_{obs}, deprived of any buffer input, can afterward be expressed through the simplified eq 3:

$$k'_{obs} = k_0 + k_H[H^+] + k_{OH}[OH^-] \quad (3)$$

The unknown kinetic quantities k_0, k_H, and k_{OH} for the forward and backward epimerization of **1** have then been obtained (see Table 3S and Figure 3S of the Supporting Information) by fitting the scatter plot data pH vs k'_{obs} to eq 3 according to a nonlinear regression procedure. The reliability of such a procedure was supported by the achievement of really good correlation coefficients (from the treatment with water data, nine data points: R^2 = 0.985 for the $\beta \rightarrow \alpha$ epimerization,

dx.doi.org/10.1021/jo102392p |J. Org. Chem. 2011, 76, 4831–4840

Table 1. Pseudo-First-Order Epimerization Rate Constants Measured at Different Temperatures and pHs in Either Buffered Ternary Aqueous Mixtures or Unbuffered Solutions of Different Ionic Strength

			pH								
		T (°C)	2.55	3.01	3.80	3.92	5.50	6.00	6.87	7.28	8.25
$k_{\alpha\rightarrow\beta}$ ($\times 10^4$ s^{-1})	phosphate buffer (10 mM)	10	2.1[a]	1.1[a]	0.8[a]		0.3[a]	0.5[c]	1.3	2.5	8.1
		20	4.8[a]	2.7[a]	1.7[a]		0.7[a]	1.2[c]	2.3	6.5	21.8
		26	8.9	4.5	2.6[a]						
		30	10.8	6.8[b]	3.5		1.8		6.7		
		35	16.3	12.3	5.1[b]						
		40	23.4	15.9	7.4	5.7	4.6	7.3	17.8	29.4	81.4[d]
		45	44.4	26.8	10.6[b]						
		50	58.5[a]	43.0[a]	15.3	9.2	10.2	12.4	55.8	61.8[a]	162.3[a]
		60			32.4		23.2				
		70					44.9				
	NaCl (1 mM)	20							3.2		
	NaCl (10 mM)	20							2.5		
	NaCl (100 mM)	20							2.7		
	no addition of buffers and salts	30							5.6		
		35							9.4		
		40							13.8		
$k_{\beta\rightarrow\alpha}$ ($\times 10^4$ s^{-1})	phosphate buffer (10 mM)	10	4.2[a]	2.2[a]	1.5[a]		0.5[a]	0.9[c]	2.8	4.4	12.0
		20	9.9[a]	5.5[a]	3.3[a]		1.4[a]	2.3[c]	4.7	11.8	33.5
		26	18.0	9.2	5.2[a]						
		30	22.1	14.1[b]	7.1		3.6		14.6		
		35	33.4	25.7	10.5[b]						
		40	49.9	33.4	15.4	11.9	9.5	15.5	39.8	62.5	173.9[d]
		45	91.9	56.3	22.8[b]						
		50	127.3[a]	90.9[a]	33.4	19.9	21.9	27.0	125.4	136.8[a]	380.2 [a]
		60			73.3		51.0				
		70					99.0				
	NaCl (1 mM)	20							6.3		
	NaCl (10 mM)	20							5.2		
	NaCl (100 mM)	20							5.4		
	no addition of buffers and salts	30							11.8		
		35							19.8		
		40							29.6		

[a] Data extrapolated by correlations $1/T$ vs $\Delta G^{\ddagger}/T$. [b] Data interpolated by correlations $1/T$ vs $\Delta G^{\ddagger}/T$. [c] Data interpolated by correlations pH vs $\Delta G^{\ddagger}$. [d] Data extrapolated by correlations pH vs $\Delta G^{\ddagger}$. Errors associated to the kinetic data from DHPLC were ≤12%.

R^2 = 0.987 for the α→β interconversion, respectively; from the treatment with WA solution data, nine data points: R^2 = 0.988 for the β→α epimerization, R^2 = 0.991 for the α→β interconversion, respectively).

From the above results, it is evident that, irrespective of the considered solvent reference (i.e., pure water or WA solution), the specific base-catalysis is much more efficient than the acid-catalysis. Furthermore, the specific base-catalysis operated by OH^- also appeared to be much more effective than the general catalysis performed by the buffer anions. A quite similar behavior was already reported for the breakdown of several aryl hemiketals of α-bromoacetophenone.[23a] On the contrary, the specific acid-catalysis by H^+ was shown to be quite similarly efficient to the corresponding general acid-catalysis by H_3PO_4. About the constant term k_0, the fitting procedure afforded values very close to those expected for the catalytic contributions coming from the chromatographic stationary phase (1.2×10^{-3} s^{-1} from water data, 1.0×10^{-3} s^{-1} from WA solution data for the forward k_0 term and 5.50×10^{-4} s^{-1} from water data, 4.7×10^{-4} s^{-1} from WA solution data for the backward k_0 term by the fitting procedure against the SPC quantities 1.10×10^{-3} and 4.68×10^{-4} s^{-1} previously obtained as effects of the stationary phase for the same column,[18] respectively), so that such an input was assumed to have, in its essence, just this origin. To get a more detailed picture of the catalytic contributions given to k_{obs} by the single H^+, OH^-, H_3PO_4, $H_2PO_4^-$, and HPO_4^{2-} species as a function of their efficiency (i.e., the related value of the second-order rate constant) and concentration, we calculated for the explicit temperature of 40 °C their individual contribution at each established pH in the 2−8 range by splitting eq 2 into the respective components. The results obtained with reference to thermodynamic data coming from both pure water and WA solution are collected in Table 4S of the Supporting Information and plotted in Figures 3 and 4 (only data related to the **1β→1α** interconversion). Obviously, the inevitable errors, in absolute sense, involved by the above exposed approximations will be

dx.doi.org/10.1021/jo102392p |J. Org. Chem. 2011, 76, 4831–4840

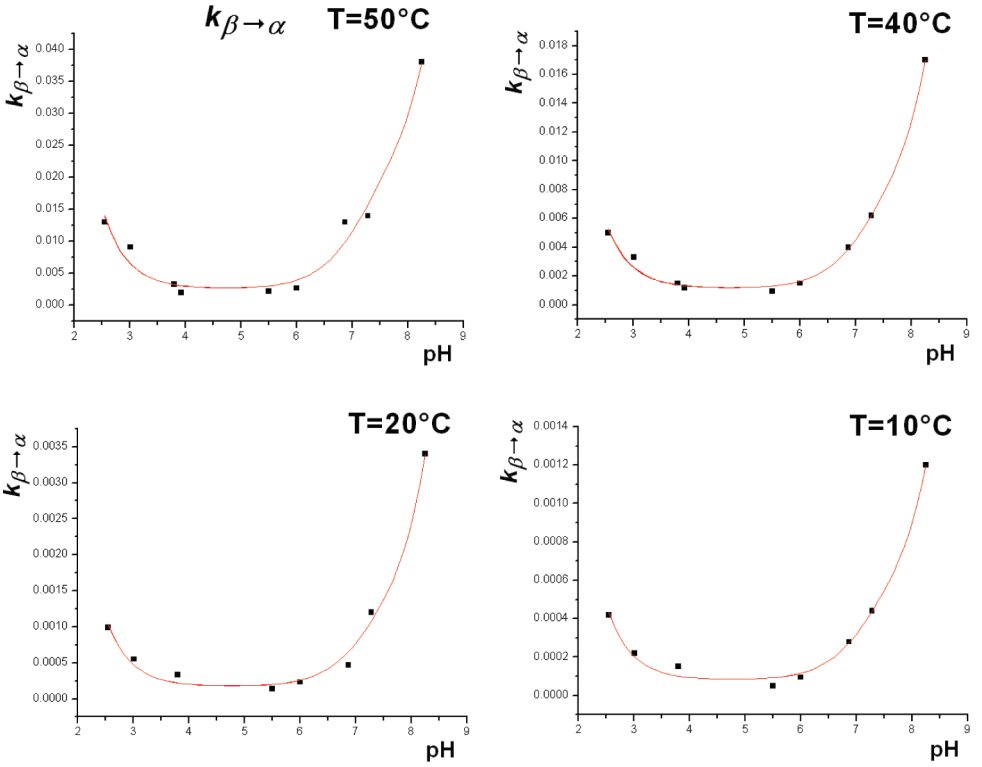

Figure 2. Rate−pH profiles of the **1*β*→1α** epimerization as a function of temperature, in the 10−50 °C range.

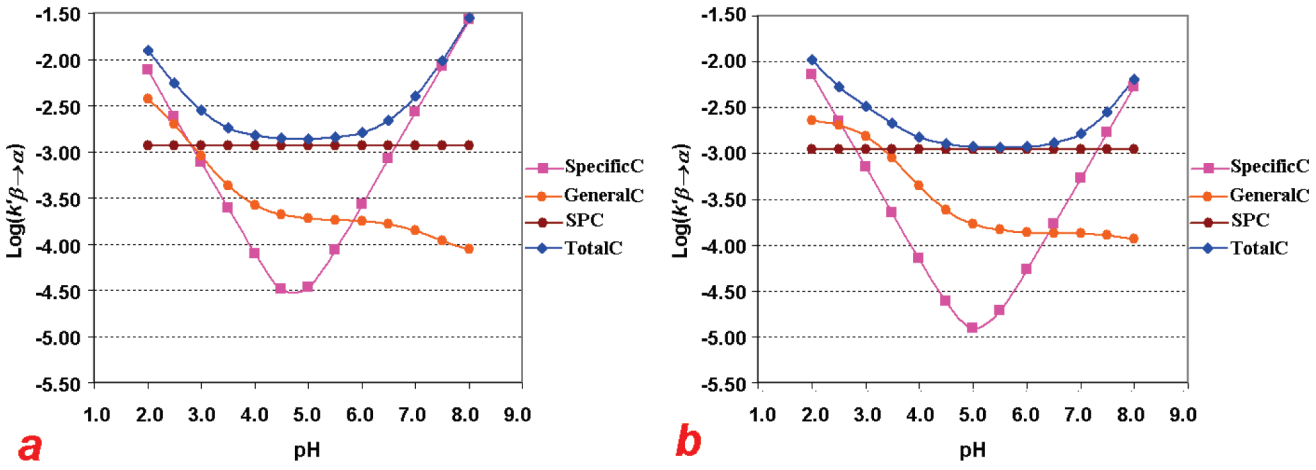

Figure 3. Calculated specific (SpecificC) and general (GeneralC) catalytic contributions to the k_{obs} pseudo-first-order rate constant at 40 °C for the **1*β*→1α** epimerization as a function of pH in water−acetonitrile−methanol 55:35:10 (v/v/v) solutions buffered by 10 mM sodium phosphate salts. With SPC and TotalC are also reported (i) the constant catalytic contribution afforded to k_{obs} by the chromatographic stationary phase and (ii) the sum of the three contributions SpecificC, GeneralC, and SPC at each considered pH. (a) Data from pK_{a1}, pK_{a2} and pK_w in water. (b) Data from pK_{a1}, pK_{a2}, and pK_w in WA−solution.

reflected in a systematic, although moderate, way on the whole explored range of pH; nevertheless, the so-evaluated buffer effects, translated to the real case of biological fluids where much more active species are certainly present, should retain an important and explanatory relevance.

Inspection of the results coming from the medium treated as WA-solutions reveals the following points: (i) Below pH 4.5, a greater catalytic contribution comes from both H^+ and H_3PO_4 than from $H_2PO_4^-$. In particular, the inputs from the two acidic species show a prevalence of the general acid on the specific one up to pH 2.5. Under this value the trend is inverted. (ii) In the 4.5−6.5 pH range, $H_2PO_4^-$ plays the prevalent catalytic role, with minimal additive contributions coming from the acidic H^+ and HPO_4^{2-} and basic OH^- species in the more restricted 5−6 pH range. (iii) In the pH interval from 6.5 to 8, the double-charged species HPO_4^{2-} does not show any input, while a residual provision of catalysis is again afforded by the $H_2PO_4^-$ ions. Instead, a completely dominant and growing catalytic effect is displayed by OH^- ions. One conclusion that can be made is that the base-promoted epimerization of **1** is largely preferred over the acid-promoted epimerization, the first

dx.doi.org/10.1021/jo102392p |*J. Org. Chem.* 2011, 76, 4831–4840

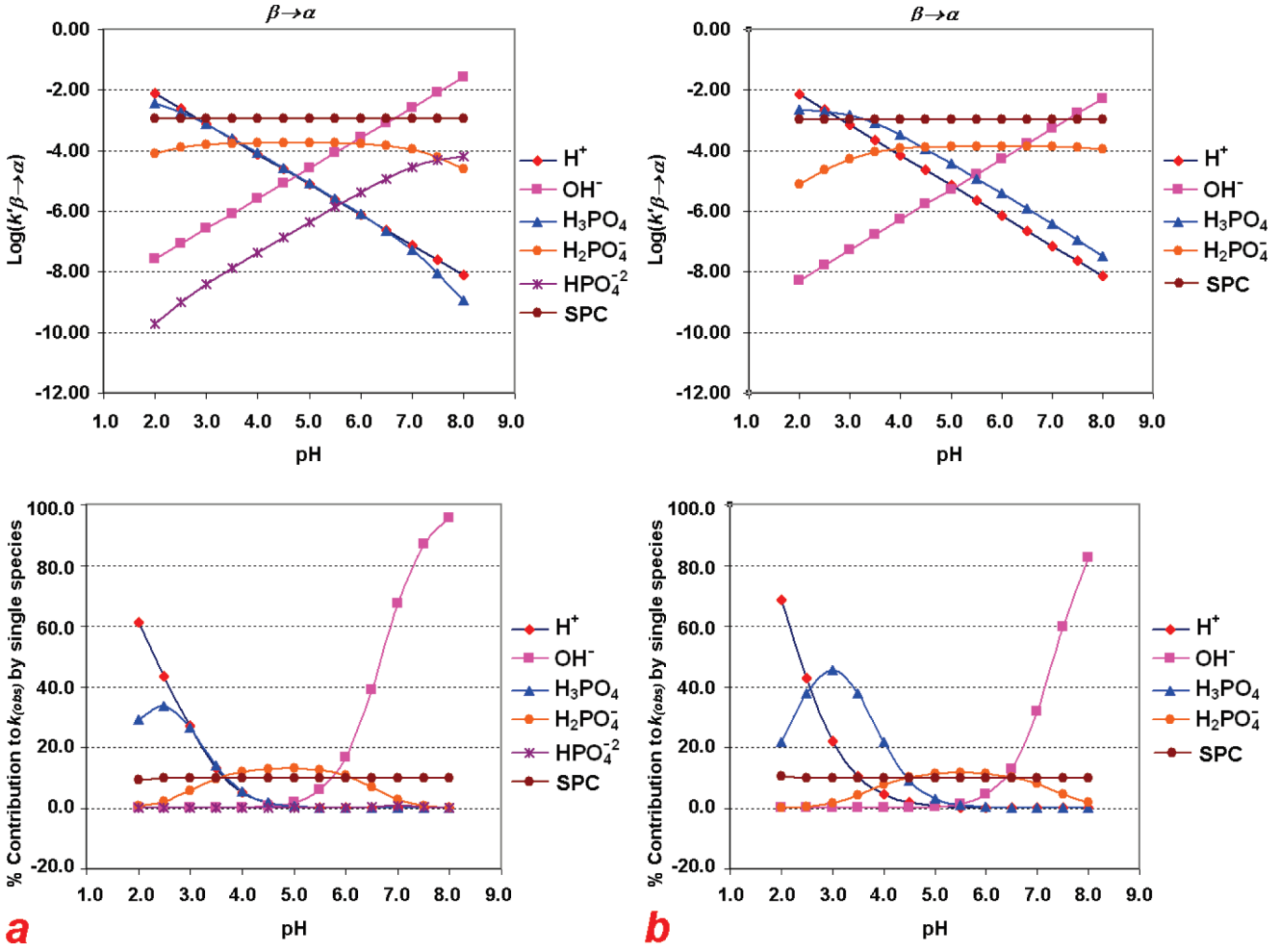

Figure 4. Calculated contributions of single catalytic species to the k_{obs} pseudo-first-order rate constant at 40 °C for the **1α**→**1*β*** epimerization as a function of pH in water−acetonitrile−methanol 55:35:10 (v/v/v) solutions buffered by 10 mM sodium phosphate salts. Top view: logarithms of the absolute contributions to k_{obs} vs pH. Bottom view: percent contributions to k_{obs} vs pH. (a) Data from pK_{a1}, pK_{a2}, and pK_w in water. (b) Data from pK_{a1}, pK_{a2}, and pK_w in WA solution.

being the dominant mechanism at pH > 4.5 (in this context, it was assumed that, because of the low value of 6.2×10^{-8} M of their ionization constant, the ions $H_2PO_4^-$ act as basic species).

Molecular Modeling Calculations. To find a rational explanation of the above results we resorted to the molecular modeling calculations already performed[19] (see also the Experimental Section) on the structure of **1α**$^-$ and **1*β***$^-$ anions, as well as on that of the conjugate acids **1α** and **1*β*** in water, acetonitrile, and hexane. In all cases, their resulting geometries showed a varying, substantial degree of opening of the hemiacetal cycle. In particular, it appeared that the extent of breakdown becomes more pronounced moving from acetonitrile or water to hexane and even more in the gas phase (see Figure 5). Notably, the extent of bond cleavage of the C−O bond in α position to the hemiacetal carbon is strongly progressed in the case of **1α**$^-$ anion (70% in gas phase and 68% in water and acetonitrile), while it is less advanced for **1*β***$^-$ (51% in gas phase and 29% in water and acetonitrile). This is particularly evident when looking at the C−O atomic distances of the breaking bond in the optimized structures of **1α**$^-$ and **1*β***$^-$ and in the opened structure **3** (see Scheme 1), where the C−O bond is completely broken (Figure 5).

This evidence strongly suggests that the involvement of basic species effectively makes the hemiacetal ring in **1α** and **1*β*** ready to undergo an almost spontaneous breakdown and that the rate-limiting step of such a kinetic pathway should be the previous equilibrium of proton transfer from the substrate to the basic catalyst (step [1]a of Scheme 1), rather then the ring-opening in the anionic intermediates **1α**$^-$ and **1*β***$^-$ (step [1]b).

Hemiacetal Ring-Opening Mechanism. As reported elsewhere,[23] we faced a scenario typical of hemiacetals and hemiketals derived from strongly acid alcohols, whose pK_a values approach or are smaller than ~13. The conjugate bases resulting by deprotonation of these latter species manifest, in fact, a resolute aptitude to be very good leaving groups. Consequently, in the base-catalyzed mechanism, as soon as they are formed, they may undergo breakdown faster than they can reprotonate and revert to the original neutral form. Some relevant examples of hemiketals deriving by parent alcohols with pK_a values smaller or close to the above limit are given by the 2,2,2-trifluoroethyl, 4-methoxyphenol, and 3-chlorophenol hemiketals of α-bromoacetophenone[23a] (pK_a of the parent alcohols: 12.37, 10.20, and 9.02). By using two commercial software programs,[24] we estimated for the alcoholic function resulting from the breakdown of the two epimers of **1** (i.e., the conjugate acid **3** of the anionic

dx.doi.org/10.1021/jo102392p |*J. Org. Chem.* 2011, 76, 4831–4840

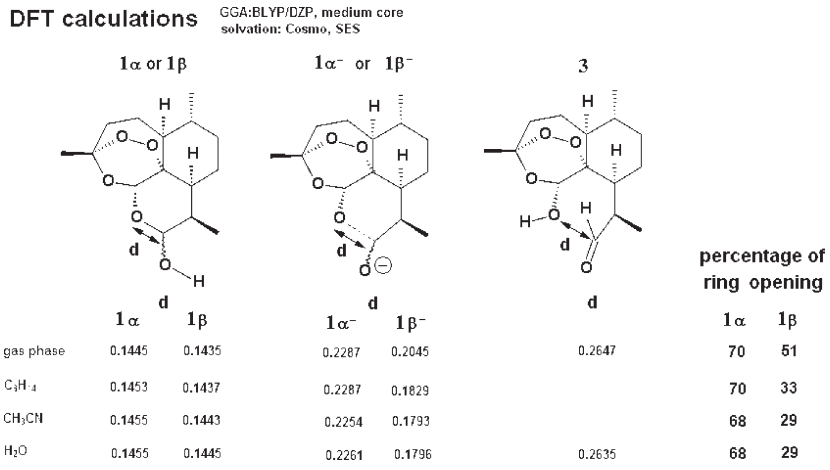

Figure 5. Extent of bond cleavage of the C−O bond, in α position to the hemiacetal carbon of **1**, estimated by DFT calculations (for details, see the Experimental Section). Interatomic distances are expressed in nm.

Scheme 1. Base- (Pathway [1]) and Acid-Catalyzed (Pathway [2]) Breakdown of 1α and 1*β*

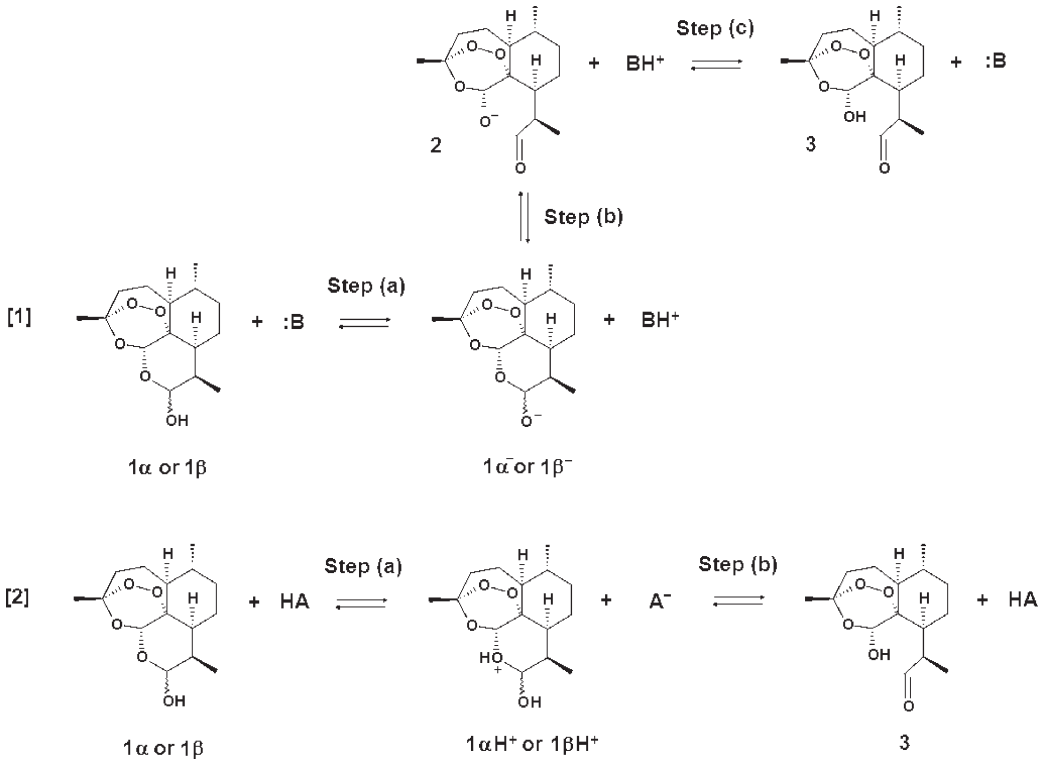

intermediate **2** reported in Scheme 1) the pK_a values of 11.32[24a] and 12.42.[24b] Apart from the small difference between these values, they were always smaller than 13. Thus, this finding also gave further support to the hypothesis that, in the base-catalyzed epimerization of **1**, deprotonation is the rate-limiting step. In tight analogy with the results found in the absence of buffers (see Table 1Sb of the Supporting Information), the van't Hoff analysis carried out on the activation barriers related to the first-order rate constants given in Table 1 indicated that the time-limiting step of the epimerization of **1** is only slightly dependent on the temperature; in fact, at all the considered pH values, the calculated variations of activation entropy, i.e., $\Delta S^{\ddagger}_{\beta-\alpha}$ and $\Delta S^{\ddagger}_{\alpha-\beta}$, have small negative values (-26 ± 3 and -23 ± 3 e.u. are the averaged amounts, respectively; see Table 1Sa of the Supporting Information). At the same time, according to the superimposed existence of different catalytic mechanisms and species operating in the explored pH range, the calculated activation enthalpies $\Delta H^{\ddagger}_{\beta-\alpha}$ and $\Delta H^{\ddagger}_{\alpha-\beta}$ showed varying values as a function of pH. These, in fact, gave place to bell-shaped profiles that achieved the maximum in the restricted 5.0−6.5 pH range (see Figure 6). Interestingly, upon pH variation, more negative $\Delta S^{\ddagger}$ values correspond to smaller values of $\Delta H^{\ddagger}$. As a consequence, at a given temperature, these opposite trends restrain the difference between the maximum and minimum value that $\Delta G^{\ddagger}$ may assume in response to pH changes.

To conclude the kinetic study on the epimerization of **1**, we performed a van't Hoff analysis on the activation barriers related

dx.doi.org/10.1021/jo102392p |*J. Org. Chem.* 2011, 76, 4831–4840

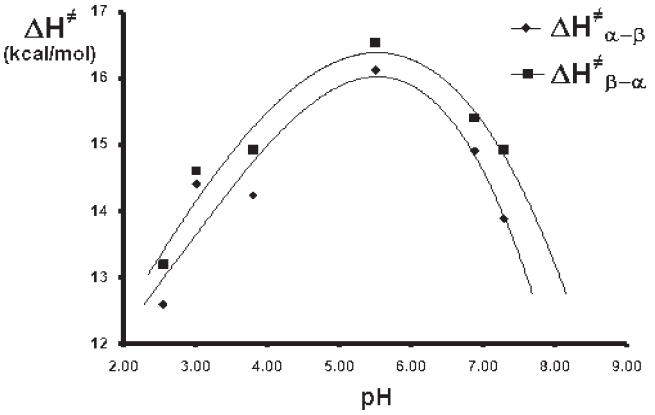

Figure 6. Activation enthalpies (kcal mol^{-1}) of the **1*β***→**1α** (top curve) and **1α**→**1*β*** epimerizations (bottom curve) expressed as a function of pH in water−acetonitrile−methanol 55:35:10 (v/v/v) solutions buffered by 10 mM sodium phosphate.

to the first-order rate constants measured at each considered pH value in the 2−8 range. Considering the results on both forward and backward epimerization of **1** (see Table 1Sa of the Supporting Information), it was pointed out that, in the examined ternary hydro-organic mixture, the enthalpic activation barriers for the **1α**→**1*β*** isomerization are in all cases lower than those for the opposite conversion (i.e., $\Delta\Delta H^{\ddagger} = \Delta H^{\ddagger}_{\alpha-\beta} - \Delta H^{\ddagger}_{\beta-\alpha} < 0$), and this is in contrast with the corresponding experimental $\Delta\Delta G^{\ddagger}$ values that, in the range of the explored temperatures, are always greater than zero (that is, the related $K_{\alpha/\beta}$ equilibrium constants are >1). However, the right correspondence is promptly restored when entropic contributions are taken into account. Such results suggest that the experimental relative abundance of the **1α** and **1*β*** epimers in the ternary medium is essentially entropic in origin or else the $K_{\alpha/\beta}$ constant would be smaller than one by the effect of the enthalpic term only. This is consistent with a differential solvation of the transition states developed during the rate-limiting step of deprotonation, which may be predicted to be significantly more effective than that involving the related ground states. Such transition states feature advanced degrees of proton transfer (more than 80%) toward the catalyzing base[23a] (i.e., they have a strong anionic character), in an extent modulated by the hemiacetal acidity. Therefore, the different acidity that we found[19] for **1α** and **1*β*** may easily accounts for the observed differential effect on entropy; this suggests the formation of stronger interactions of the solvent molecules (which, then, reduce their entropy more distinctly) with the transition state related to **1α** compared to **1*β***, because the more acidic epimer should clearly undergo a more advanced degree of proton transfer.

Half-Life Times Prediction in Physiological Fluids. With the above kinetic information on the $\beta \rightleftarrows \alpha$ interconversion of **1** in hand, it was possible to calculate approximate half-life times ($t_{1/2}$) for the **1α** and **1*β*** species allowed to equilibrate within physiological fluids found in different human organs or tissues at 40 °C (see Table 4S of the Supporting Information). Because in these estimations we considered H^+ and OH^- ions as the exclusive catalytic species, the calculated $t_{1/2}$ times have to be considered as upper limit values, which could therefore be further reduced by general acid and basic species present in such media. As an approximation, it was assumed that, in such fluids, the second-order rate constants k_H and k_{OH} at 40 °C were the same as determined in the ternary mixture. By inspection of the results collected in Table 5S of the Supporting Information, we concluded that in all the considered physiological media, with the exception of saliva and urine, the calculated half-life times of **1** were smaller than 10 min. This clearly means that, from a kinetic point of view, a significant presence of both epimers, corresponding to the equilibrium ratio $K_{\alpha/\beta}$, would be found after about 1 h in such biological systems, irrespective of the isomeric purity at which **1** would have been administered. From a thermodynamic point of view, however, it should be also taken into account that the relative abundance of **1α** and **1*β*** could be influenced by the presence of species (typically, globular proteins) able to form complexes of different stability, thus shifting the **1α**/**1*β*** equilibrium position.

CONCLUSIONS

The present study was conceived to achieve information about kinetic and mechanistic features of the **1α**/**1*β*** equilibration by both experimental and theoretical approaches. As expected, the epimerization rates were found to be sensitive to both acids and bases. However, in the solvent systems tested, the specific base-catalysis was demonstrated to be much more effective than the specific acid-catalysis, as well as more influencing than the corresponding general catalysis in the analyzed buffered ternary mixture. Instead, acid-catalysis by both specific and general species (H^+ and H_3PO_4, respectively) was shown to be of quite similar efficiency and dominant at pH < 4.5. In such a system, the epimerization rates were measured and analyzed as a function of ionic strength, pH, and temperature, and it was found that a base-catalyzed mechanism was responsible for the epimerization in quantitative terms at pH values greater than 4.5. Moreover, theoretical calculations suggested that the rate-limiting step of the process was not the ring-opening of the cyclic hemiacetal but the previous deprotonation equilibrium of the individual epimers. By dividing the entropic and enthalpic contributions to the free energy activation barriers calculated as function of pH for both the forward and backward epimerizations, it was also found that the observed α/*β* concentration ratio is entropic in origin, according to a differential solvation of the transition states in the rate-limiting step of proton transfer. This, in turn, can be related to the different acidity already found[19] for **2α** and **2*β***.

We believe that the present results on the stereolability of **1** may contribute to shed some light on the mechanism of action and/or bioavailability of the drug at molecular level and represent a promising starting point for future studies and rational design of semisynthetic artemisinin derivatives.

EXPERIMENTAL SECTION

Chromatography. Analytical liquid chromatography was performed using a Waters model 2695 HPLC separation module coupled with a Waters 996 photodiode array detector. Chromatographic data were collected and processed using Empower2 software (Waters). Variable-temperature HPLC (DHPLC) was performed by using a laboratory-made thermally insulated container cooled by the expansion of liquid carbon dioxide (CO_2). Flow of liquid CO_2 and column temperature were regulated by a solenoid valve, thermocouple, and electric controller. Temperature variations after thermal equilibration were within ±0.2 °C.

Normal-phase HPLC for the classic batchwise approach was performed on a Reprosil Si 120, 3 μm (150 × 4.6 mm i.d.) column with a mobile phase made up of *n*-hexane−ethanol 97:3 (v/v), delivered at

1.0 mL min^{-1}, and UV detection at 214 nm (T = 25 °C). Reversed-phase HPLC was performed on a C_{18} symmetry, 3.5 μm (100 × 4.6 mm i.d.) column, with a mobile phase composed of water−acetonitrile−methanol 55:35:10 (v/v/v) buffered to apparent pH 5.6 using 10 mM sodium phosphate, delivered at 1.0 mL min^{-1}, and UV detection at 214 nm (T = 5 °C).

All the DHPLC experiments were performed on a C_{18} symmetry, 3.5 μm (75 × 4.6 mm i.d.) column, with a ternary hydro-organic mobile phase delivered at 1.0 mL min^{-1} and UV detection at 214 nm. For the study of the effects of pH and temperature on the rate constants, a ternary mobile phase consisting of water−acetonitrile−methanol 55:35:10 (v/v/v), at controlled temperatures in the range of 10−70 °C was tested. Solutions of **1** (0.25−1.0 mg mL^{-1}) in the mobile phase were buffered to apparent pH values ranging from 2.6 to 8.3 using 10 mM sodium phosphate. Aliquots of 10−20 μL were injected. Increasing concentrations of sodium phosphate buffer inside the range 10−200 mM were used in the study addressed to quantify the catalytic role of each buffer's component (see Table 2S and Figure 2S of the Supporting Information for details about the employed concentrations). Sodium chloride (1, 10, and 100 mM) replaced sodium phosphate in the ternary mobile phase water−acetonitrile−methanol 55:35:10 (v/v/v) in the study of the role of ionic strength.

Simulation of Dynamic Chromatograms. Simulations of experimental dynamic chromatograms were performed by using the Auto DHPLC y2k laboratory-made computer program,[21] which implements both stochastic and theoretical plate models[20] and may take into account all types of first-order interconversions as well as tailing effects. In the present paper, all simulations were carried out by using the stochastic model and taking tailing effects into consideration. The rate constants in the mobile phase were properly set in order to obtain a **1α**/**1β** ratio consistent with the thermodynamic $K_{\alpha/\beta}$ ratio experimentally measured in the same media by ^{1}H NMR, according to a procedure reported elsewhere.[18]

Molecular Modeling Calculations. Geometries of **1α**, **1β**, **1α**$^-$, **1β**$^-$, and **3** were optimized at the SCF level by DFT calculations run with the Amsterdam Density Functional (ADF) package v. 2007.01. The employed method was the GGA-BLYP/DZP medium core basis set. All of the relative solvation energies in hexane, acetonitrile, and water were computed with the same program by the COnductor like Screening MOdel (COSMO), with the cavity defined according to the Solvent Excluding Surface (SES) algorithm.

■ ASSOCIATED CONTENT

Supporting Information. Activation parameters for the forward and backward first-order epimerization of **1**. Second-order rate constants based on specific and general acid and basic catalysis. Contributions to the forward and backward pseudo-first-order epimerization rate constants. Dynamic chromatograms digitalized by ref 17. Cartesian coordinates of **1α**, **1β**, **1α**$^-$, **1β**$^-$, and **3**. This material is available free of charge via the Internet at http://pubs.acs.org.

■ AUTHOR INFORMATION

Corresponding Author

*E-mail: (F.G.) francesco.gasparrini@uniroma1.it; (M.P.) marco.pierini@uniroma1.it.

■ ACKNOWLEDGMENT

We acknowledge financial support from FIRB [research program: Ricerca e Sviluppo del Farmaco (CHEM-PROFARMA-NET), grant no. RBPR05NWWC_003] and from Sapienza Università di Roma, Italy (funds for selected research topics 2008−2010).

■ REFERENCES

(1) Guidelines for the treatment of malaria. World Health Organization, 2009.

(2) O'Neill, P. M. *Expert Opin. Invest. Drugs* **2005**, *14*, 1117–1128.

(3) (a) O'Neill, P. M.; Posner, G. H. *J. Med. Chem.* **2004**, *47*, 2945–2964. (b) Bez, G.; Kalita, B.; Sarmah, P.; Barua, N. C.; Dutta, D. K. *Curr. Org. Chem.* **2003**, *7*, 1231–1255.

(4) Posner, G. H.; Paik, I.-H.; Chang, W.; Borstnik, K.; Sinishtaj, S.; Rosenthal, A. S.; Shapiro, T. A. *J. Med. Chem.* **2007**, *50*, 2516–2519.

(5) Li, Q. G.; Peggins, J. O.; Fleckenstein, L. L.; Masonic, K.; Heiffer, M. H.; Brewer, T. G. *J. Pharm. Pharmacol.* **1998**, *50*, 173–182.

(6) (a) Pathak, A. K.; Jain, D. C.; Sharma, R. P. *Indian J. Chem., Sect. B: Org. Chem. Incl. Med. Chem.* **1995**, *34*, 992–993. (b) Haynes, R. K.; Chan, H.-W.; Lung, C.-M.; Ng, N.-C.; Wong, H.-N.; Shek, L. Y.; Williams, I. D.; Cartwright, A.; Gomes, M. F. *Chem. Med. Chem.* **2007**, *2*, 1448–1463. (c) Dhooghe, L.; Van Miert, S.; Jansen, H.; Vlietinck, A.; Pieters, L. *Pharmazie* **2007**, *62*, 900–901. (d) Jansen, F. H.; Soomro, S. A. *Curr. Med. Chem.* **2007**, *14*, 3243–3259. (e) Haynes, R. K. *Chem. Med. Chem.* **2006**, *6*, 509–537.

(7) Zhou, Z. M.; Anders, J. C.; Chung, H.; Theoharides, A. D. *J. Chromatogr.* **1987**, *414*, 77–90.

(8) Karbwang, J.; Na-Bangchang, K.; Molunto, P.; Banmairuroi, V.; Congpuong, K. *J. Chromatogr. B* **1997**, *690*, 259–265.

(9) (a) Batty, K. T.; Davies, T. M. E.; Thu, L. T.; Binh, T. Q.; Anh, T. K.; Ilett, K. F. *J. Chromatogr. B* **1996**, *677*, 345–350. (b) Batty, K. T.; Ilett, K. F.; Davis, T. M. E. *J. Pharm. Pharmacol.* **1996**, *48*, 22–26. (c) Kotecka, B. M.; Rieckmann, K. H.; Davis, T. M. E.; Batty, K. T.; Ilett, K. F. *Acta Trop.* **2003**, *87*, 371–375. (d) Batty, K. T.; Ilett, K. F.; Davis, T. M. E. *Br. J. Clin. Pharmacol.* **2004**, *57*, 529–533.

(10) (a) Navaratnam, V.; Mordi, M. N.; Mansor, S. M.; Chin, L. K.; Asokan, M.; Nair, N. K. *J. Chromatogr. B* **1995**, *669*, 289–294. (b) Navaratnam, V.; Mordi, M. N.; Mansor, S. M. *J. Chromatogr. B* **1997**, *692*, 157–162. (c) Lai, C.-S.; Nair, N. K.; Mansor, S. M.; Olliaro, P. L.; Navaratnam, V. *J. Chromatogr. B* **2007**, *857*, 308–314.

(11) (a) Sandrenan, N.; Sioufi, A.; Godbillon, J.; Netterb, C.; Danker, M.; van Valkenburg, C. *J. Chromatogr. B* **1997**, *691*, 145–153. (b) Souppart, C.; Gauducheau, N.; Sandrenan, N.; Richard, F. *J. Chromatogr. B* **2002**, *774*, 195–203.

(12) Avery, B. A.; Venkatesh, K. K.; Avery, M. A. *J. Chromatogr. B* **1999**, *730*, 71–80.

(13) Ortelli, D.; Rudaz, S.; Cognard, E.; Veuthey, J.-L. *Chromatographia* **2000**, *52*, 445–450.

(14) (a) Sabarinath, S.; Rajanikanth, M.; Madhusudanan, K. P.; Gupta, R. C. *J. Mass Spectrom.* **2003**, *38*, 732–742. (b) Rajanikanth, M.; Madhusudanan, K. P.; Gupta, R. C. *Biomed. Chromatogr.* **2003**, *17*, 440–446.

(15) Naik, H.; Murry, D. J.; Kirsch, L. E.; Fleckenstein, L. *J. Chromatogr. B* **2005**, *816*, 233–242.

(16) Liu, Y.; Zeng, X.; Deng, Y.; Wang, L.; Feng, Y.; Yang, L.; Zhou, D. *J. Chromatogr. B* **2009**, *877*, 465–470.

(17) Shishan, Z. *Chromatographia* **1986**, *22*, 77–80.

(18) (a) Cabri, W.; Ciogli, A.; D'Acquarica, I.; Di Mattia, M.; Galletti, B.; Gasparrini, F.; Giorgi, F.; Lalli, S.; Pierini, M.; Simone, P. *J. Chromatogr. B* **2008**, *875*, 180–191. (b) D'Acquarica, I.; Gasparrini, F.; Kotoni, D.; Pierini, M.; Villani, C.; Cabri, W.; Di Mattia, M.; Giorgi, F. *Molecules* **2010**, *15*, 1309–1323.

(19) Cabri, W.; D'Acquarica, I.; Simone, P.; Di Iorio, M.; Di Mattia, M.; Gasparrini, F.; Giorgi, F.; Mazzanti, A.; Pierini, M.; Quaglia, M.; Villani, C. *J. Org. Chem.* **2011**, *76*, 1751–1758.

(20) (a) Keller, R. A.; Giddings, J. C. *J. Chromatogr.* **1960**, *3*, 205–220. (b) Kramer, R. *J. Chromatogr.* **1975**, *107*, 241–252. (c) Schurig, V.; Bürkle, W. *J. Am. Chem. Soc.* **1982**, *104*, 7573–7580. (d) Bürkle, W.; Karfunkel, H.; Schurig, V. *J. Chromatogr.* **1984**, *288*, 1–14. (e) Veciana, J.; Crespo, M. I. *Angew. Chem., Int. Ed. Engl.*

1991, *30*, 74−77. (f) Jung, M. *QCPE Bull.* **1992**, *12*, 52. (g) Cabrera, K.; Jung, M.; Fluck, M.; Schurig, V. *J. Chromatogr. A* **1996**, *731*, 315–321. (h) Oxelbark, J.; Allenmark, S. *J. Org. Chem.* **1999**, *64*, 1483–1486. (i) Trapp, O.; Schoetz, G.; Schurig, V. *Chirality* **2001**, *13*, 403−414. (j) Wolf, C. *Chem. Soc. Rev.* **2005**, *34*, 595–608. (k) Trapp, O. *Anal. Chem.* **2006**, *78*, 189–198. (l) D'Acquarica, I.; Gasparrini, F.; Pierini, M.; Villani, C.; Zappia, G. *J. Sep. Sci.* **2006**, *29*, 1508–1516.

(21) (a) Alcaro, S.; Casarini, D.; Gasparrini, F.; Lunazzi, L.; Villani, C. *J. Org. Chem.* **1995**, *60*, 5515–5519. (b) Gasparrini, F.; Lunazzi, L.; Mazzanti, A.; Pierini, M.; Pietrusiewicz, K. M.; Villani, C. *J. Am. Chem. Soc.* **2000**, *122*, 4776–4780. (c) Dell'Erba, C.; Gasparrini, F.; Grilli, S.; Lunazzi, L.; Mazzanti, A.; Novi, M.; Pierini, M.; Tavani, C.; Villani, C. *J. Org. Chem.* **2002**, *67*, 1663–1668. (d) Gasparrini, F.; Grilli, S.; Leardini, R.; Lunazzi, L.; Mazzanti, A.; Nanni, D.; Pierini, M.; Pinamonti, M. *J. Org. Chem.* **2002**, *67*, 3089–3095. (e) Dalla Cort, A.; Gasparrini, F.; Lunazzi, L.; Mandolini, L.; Mazzanti, A.; Pasquini, C.; Pierini, M.; Rompietti, R.; Schiaffino, L. *J. Org. Chem.* **2005**, *70*, 8877–8883. (f) Cirilli, R.; Ferretti, R.; La Torre, F.; Secci, D.; Bolasco, A.; Carradori, S.; Pierini, M. *J. Chromatogr. A* **2007**, *1172*, 160–169.

(22) (a) Subirats, X.; Rosés, M.; Bosch, E. *Sep. Purif. Rev.* **2007**, *36*, 231–255. (b) Rosés, M.; Bosch, E. *J. Chromatogr. A* **2002**, *982*, 1–30. (c) Bosch, E.; Bou, P.; Allemann, H.; Rosés, M. *Anal. Chem.* **1996**, *68*, 3651–3657. (d) Bosch, E.; Espinosa, S.; Rosés, M. *J. Chromatogr. A* **1998**, *824*, 137–146. (e) Espinosa, S.; Bosch, E.; Rosés, M. *Anal. Chem.* **2000**, *72*, 5193–5200.

(23) (a) McClelland, R. A.; Kanagasabapathy, V. M.; Mathivanan, N. *Can. J. Chem.* **1991**, *69*, 2084–2093. (b) Sorensen, P. E.; Jencks, W. P. *J. Am. Chem. Soc.* **1987**, *109*, 4675–4690. (c) Sorensen, P. E.; Pedersen, K. J.; Kanagasabapathy, V. M.; McClelland, R. A. *J. Am. Chem. Soc.* **1988**, *110*, 5118–5123.

(24) (a) ACD/Labs Package V. 6.00, (pKa DB Module), 90 Adelaide Street, West Toronto, Ontario M5H 3V9, Canada. (b) Marvin 4.1.1.3, 2007, ChemAxon (http://www.chemaxon.com). These packages were used to draw and calculate pK_a values of hemiacetals.